ACS OMEGA

Article

http://pubs.acs.org/journal/acsodf

Formation of $TbPc_2$ Single-Molecule Magnets' Covalent 1D Structures via Acyclic Diene Metathesis

Alessandro Pedrini,[†] Mauro Perfetti,[‡] Matteo Mannini,[‡] and Enrico Dalcanale*[,†]

[†]Dipartimento di Scienze Chimiche, della Vita e della Sostenibilità Ambientale & INSTM RU of Parma, Università degli Studi di Parma, Parco Area delle Scienze 17/A, 43124 Parma, Italy

[‡]Dipartimento di Chimica "Ugo Schiff" & INSTM RU of Firenze, Università degli Studi di Firenze, Via della Lastruccia 3-13, 50019 Sesto Fiorentino, Italy

Supporting Information

ABSTRACT: We present here a reaction scheme to connect $TbPc_2$ single-molecule magnets into 1D architectures using acyclic diene metathesis. To investigate the impact of the bonding through aliphatic chains on the magnetic properties of $TbPc_2$, we isolate and characterize the dimeric species obtained as one of the products of the reaction. Remarkably, the magnetic properties are only slightly modified after the formation of the bond between molecules, enlightening the great potential of this reaction scheme.

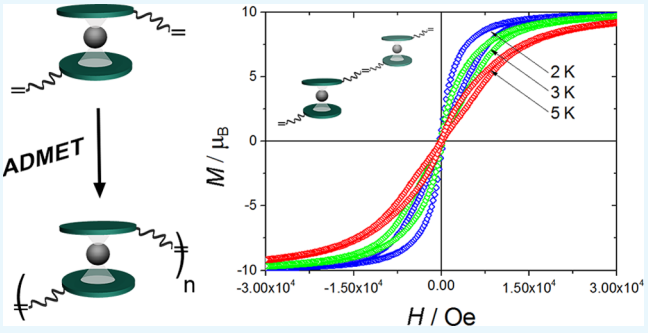

INTRODUCTION

In recent years, single-molecule magnets (SMMs), which exhibit slow magnetization relaxation of purely molecular origin, have attracted increasing interest.[1] At sufficiently low temperatures, these coordination compounds are capable to retain magnetization in the absence of external magnetic field for long time,[2] thus allowing considering each molecule as an alternative bit for data storage.[3] Quantum effects, like resonant quantum tunneling, observed in those systems in the bulk[2] and at the nanoscale,[4] have more recently fascinated molecular magnetism community for the use in innovative molecular devices.[5]

In 2003, Ishikawa and co-workers reported that lanthanide phthalocyanine double-deckers ($LnPc_2$'s), sandwich-type complexes constituted by two phthalocyaninato ligands complexing a lanthanide (III) ion, behave as magnets at a single-molecule level.[6] Their huge magnetic anisotropy is given by a highly axial ligand field (LF) produced by an (idealized) square-antiprismatic coordination geometry (D_{4d}-symmetry).[7] $LnPc_2$'s are characterized by structural robustness and versatility, which allow a fine-tuning of their magnetic properties either by replacing the metal ion or by varying the LF through ligand modification. The larger energy separation between the ground and the first excited state in the terbium derivative matches the requisites for a strong single-molecule-magnet behavior, ruling $TbPc_2$ as the most promising molecule among the $LnPc_2$ series.[8] Furthermore, the introduction of peripheral functional groups on one or both ligands is a powerful strategy to alter the relaxation dynamics, as demonstrated by Torres and co-workers who reported a record anisotropy barrier of ca. 938 K for $TbPc_2$ with OC_6H_4-p-^{t}Bu substituents.[9] However, all of the efforts to increase the effectiveness of these SMMs are frustrated by the presence of a highly favored relaxation pathway, namely, the quantum tunneling of magnetization (QTM),[10] which is intimately related to the single-ion nature of $LnPc_2$.[11]

As indicated by Wernsdorfer's pioneering work on supramolecular dimers, the interconnection of SMM centers is a powerful tool to alter their relaxation dynamics.[12] To date, different 1D, 2D, and 3D structures have been prepared through the assembly of SMMs mainly via coordination with proper ligands,[13] but the behavior of $TbPc_2$ in similar organized structures is still unexplored. As the synthesis of chemically connected SMMs is a relevant step toward realization of innovative materials,[13e] it is necessary to define procedures to link SMMs avoiding the quenching of the magnetic properties, which are often very sensitive to the chemical environment.[14]

A chemical approach to tune the magnetic properties of lanthanides is to couple these elements with delocalized radicals that can interact quite strongly with the partially shielded 4f-electrons. A strong influence of the coupling between lanthanides and radicals was indeed observed in both single chains[15] and molecular dimers.[16] In these systems, the relaxation dynamics is often ruled by the strong interaction that sometimes is able to cause opening of hysteresis and ordering at low temperatures.[15e] Interestingly, Wang and co-workers reported that also phthalocyanine-based sandwich-type dysprosium and yttrium complexes highly benefit from the formation of π-bridged dimers, due to mitigation of QTM.[17]

Received: December 23, 2016
Accepted: February 2, 2017
Published: February 13, 2017

DOI: 10.1021/acsomega.6b00546
ACS Omega 2017, 2, 517−521

Herein, we report the first example of $TbPc_2$ organization in covalent 1D structures, in particular oligomeric chains obtained by acyclic diene metathesis (ADMET).[18] Kobayashi and co-workers have already successfully applied this reaction to metallated phthalocyanines.[19] Although it shows some similarity with the more common ring-opening metathesis polymerization, ADMET is less active and gives rise to polymers with lower molecular weight, but it can be applied to a broader range of monomers. Like other metathesis reactions, ADMET proceeds under thermodynamic equilibrium and product formation must be favored by byproduct removal, which can be simplified using terminal olefins that evolve gaseous ethylene from the reaction. Terminal double bonds are among the few functional groups capable to survive harsh conditions required for $TbPc_2$ synthesis.[20]

RESULTS AND DISCUSSION

On the basis of these considerations, a homoleptic bis-ω-alkenyl $TbPc_2$ monomer (**3**) was synthesized from the corresponding monofunctionalized phthalocyanine (**2**; Scheme 1, for characterizations see Figures S1−S8). Phthalocyanine **2** was obtained by Williamson reaction between 11-bromo-1-undecene and phthalocyanine **1** bearing one hydroxy group.

Double-decker formation was carried out by the reaction of phthalocyaninato ligand **2** with terbium (III) acetylacetonate hydrate in 1-hexadecanol at 180 °C in the presence of lithium methoxide.[21] Repeated purifications by column and preparative thin-layer chromatography (TLC) afforded $TbPc_2$ **3** as a mixture of constitutional isomers in 49% yield. The formation of the desired complex was confirmed by the presence of the molecular peak in the matrix-assisted laser desorption ionization time-of-flight (MALDI-TOF) spectrum (Figure S7).

ADMET oligomerization of **3**, in the presence of a second-generation Grubbs catalyst, was initially performed in dichloromethane at room temperature with a monomer concentration of 2.4 mM. Under these conditions, the product of the intramolecular reaction between the two ω-alkenyl chains (**3′**, Scheme 1) was found to be the major component of the reaction mixture, as indicated by MALDI-TOF analysis (Figure 1a). To maximize the formation of intermolecular oligomers, the monomer concentration was increased by an order of magnitude ([**3**] = 24 mM). The reaction time was also incremented from 24 to 72 h, and 1,2-dichloroethane (DCE) was chosen as a solvent to reduce solvent loss by evaporation. MALDI-TOF analysis of the resulting mixture (Figure 1b) revealed the formation of oligomeric structures (up to pentamers). To simplify the magnetic characterization and isolate one contribution, we isolated the major component, $TbPc_2$ dimer **4**, by preparative TLC (yield of **4** ≈ 23%). MALDI-TOF characterization of **4** revealed the presence of a tiny amount of impurities, identifiable as the monomer and the trimer (Figure S8). The magnetic properties of **4** were studied without further purification.

Preliminary magnetic characterization of $TbPc_2$ dimer **4** was performed with standard dc magnetic techniques. The χT saturation value at room temperature (Figure S9) is close to the value of two independent Tb^{3+} ions ($^7F_6$, $S = 3$, $L = 3$, $J = 6$, $g_J = 3/2$) and two $S = 1/2$ delocalized radicals (24.39 emu K mol^{-1}), confirming the magnetic purity of the sample. The slight increase between 300 and 250 K can be due to either CF effects or the presence of a small amount of diamagnetic impurities. Conversely, the increase at low temperature ($T < 7$ K) is attributed most likely to intermolecular interactions or to

Scheme 1. Synthesis of $TbPc_2$ Oligomers

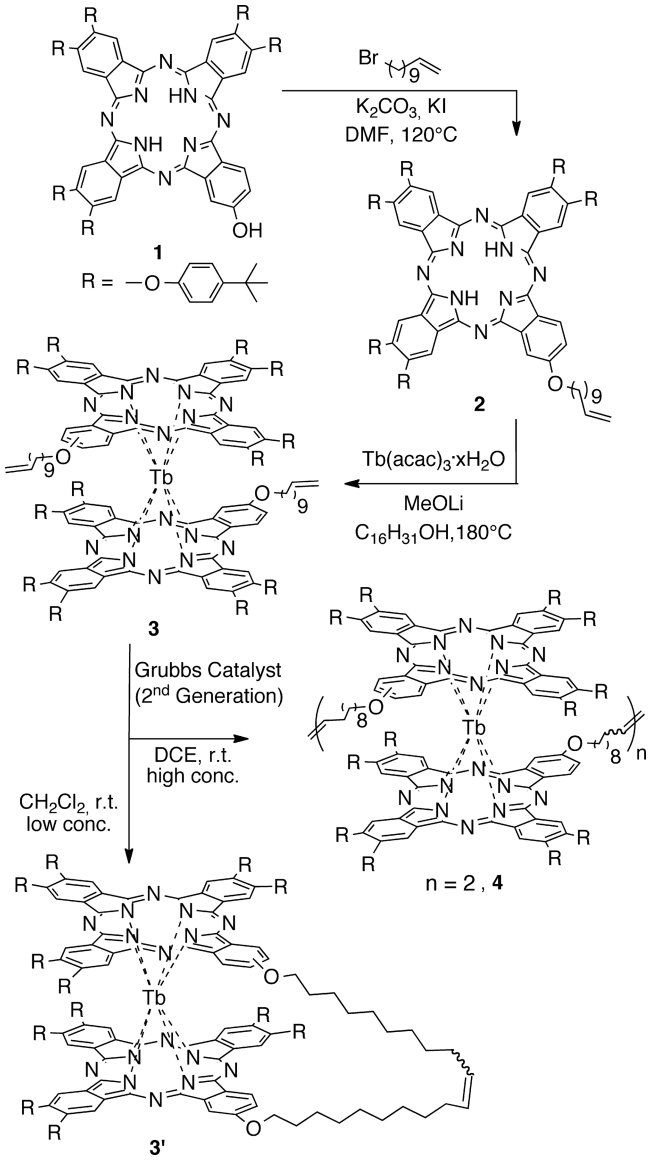

CF effects. However, an LF that reproduces the experimental increase at low T needs a very uncommon energy splitting, never observed for $TbPc_2$ derivatives and very different from the ones reported by Ishikawa for the anionic form of $TbPc_2$. In Figure S10, we reported the simulation of the χT curve using both Ishikawa parameters[7] and a set of parameters that qualitatively reproduces the low-temperature behavior. To investigate the origin of the peculiar feature of χT at low temperatures, we can foresee the use of high-dilution experiments in an YPc_2 diamagnetic matrix, to significantly enlarge the intermolecular distance and thus suppress the presence of interactions between dimers.[22]

In Figure 2, we reported the hysteresis curves measured by varying the applied field between 30 and −30 kOe (scan rate 200 Oe s^{-1}), at three different temperatures (2, 3, and 5 K). We observed the typical butterfly shape, ascribed to the presence of QTM at zero applied field. For each temperature tested, dimer **4** showed a less-pronounced hysteresis compared to that shown by the monomeric unsubstituted $TbPc_2$. However, the magnetization saturation value appeared to be comparable.[14]

DOI: 10.1021/acsomega.6b00546
ACS Omega 2017, 2, 517−521

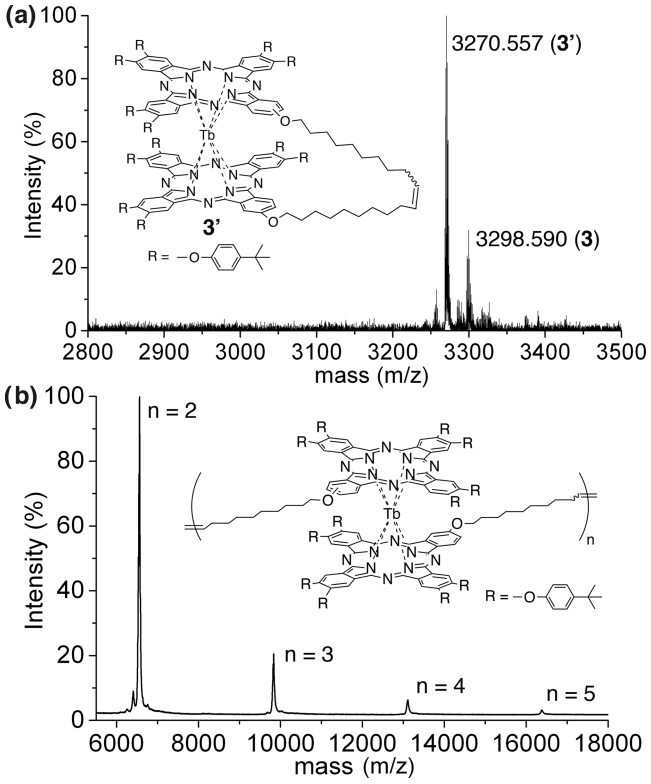

Figure 1. (a) High-resolution MALDI-TOF spectrum (expanded 2800−3500 m/z region) of the mixture obtained with [**3**] = 2.4 mM; the structure of intramolecular reaction product **3′** is shown in the inset; (b) MALDI-TOF spectrum of the crude obtained with [**3**] = 24 mM, the generic structure of oligomers is shown in the inset.

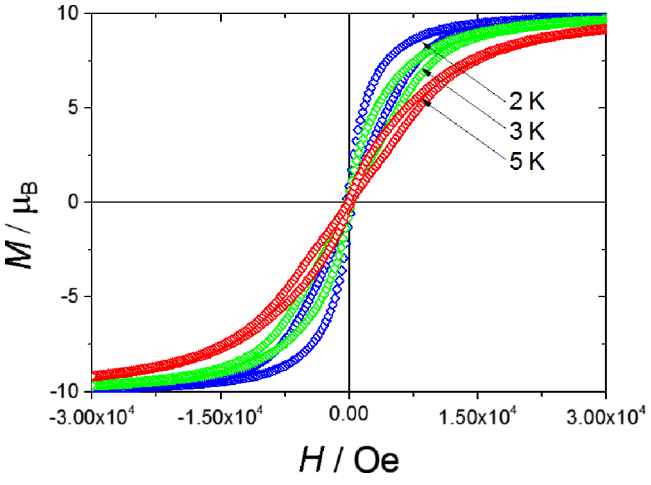

Figure 2. Temperature dependence of the hysteresis loop recorded on dimer **4**, with the field sweeping rate of 200 Oe s^{-1}.

Ac measurements were also performed to shed light on the dynamic properties of compound **4**: the magnetic susceptibility (χ) was measured at temperatures between 2 and 60 K, varying the frequency from 0.1 Hz to 10 kHz at two different static magnetic fields (H = 0 Oe and 5 kOe, Table 1). The occurrence of a maximum in the out-of-phase component (χ'') of the magnetic susceptibility indicated the presence of slow relaxation of magnetization (Figures S11−S18). The fit of the $\chi''(\nu)$ isotherms, using the Casimir and Du Pré formula (reported in Supporting Information),[23] provided the most

Table 1. Magnetic Parameters Extracted from ac Susceptibility Data under Static Applied Field for 4

	τ_0 (s)	U_{eff} (K)
H = 0 Oe	(1.03 ± 0.09) × 10^{-10}	634 ± 69
H = 5 kOe	(1.39 ± 0.06) × 10^{-11}	738 ± 49

reliable means of determining the relaxation time (τ), defined as the reversal of the frequency at which χ'' is maximum. To check if all of the magnetic centers inside the sample followed the same relaxation pathway, in Figure S19 we compared the values of the magnetic susceptibility obtained from dc measurements with the values of $\chi_T - \chi_S$ (difference between the isotherm and the adiabatic susceptibility)[22] extracted from the ac fits. The values, superimposable in the whole temperature range, confirmed that the same relaxation pathway dominates the relaxation of all magnetic centers. Moreover, the relatively high values of the distribution of relaxation times (see Figure S20) are not surprising because of the chemical strain introduced by the aliphatic chain that interconnects the molecules. In Figure S21, we reported the logarithm of the extracted relaxation times as a function of $1/T$. For H = 0 Oe, the relaxation time follows two different laws depending on the temperature range. For low temperatures, τ approaches a constant value and the relaxation dynamics is dominated by quantum tunneling of the magnetization. For high temperatures, $\ln(\tau)$ becomes linearly dependent on $1/T$ (Arrhenius behavior). When a static magnetic field of 5 kOe is applied, the quantum tunneling is suppressed and the Arrhenius behavior is extended also at lower temperatures. Coherently with the literature, we performed an Arrhenius fit of τ in the high-temperature regime, to provide an estimation of the barrier for the relaxation of the magnetization (U_{eff}) and the pre-exponential factor (τ_0). Comparing our results with the values relative to amorphous pristine $TbPc_2$,[14] it appears clear that the result of the connection between magnetic centers through the carbon chain is a slight decrease of the relaxation barrier and an increase of the pre-exponential factor. The result indicates that the connection between the molecules introduces a strain that causes lowering of the LF symmetry and thus a decrease of the relaxation barrier. However, it is worth noticing that the slow relaxation and the hysteretic behavior typical of isolated $TbPc_2$ molecules are just dumped and not quenched, confirming the robustness of the magnetic behavior of these molecules.[14,20]

CONCLUSIONS

In conclusion, we successfully applied ADMET to the oligomerization of $TbPc_2$ molecules. Selectivity among intramolecular and intermolecular reaction pathways was found to be concentration-dependent. The poor solubility of $TbPc_2$ monomer **3** limits further improvement of the oligomerization yield. Investigations on the magnetic behavior of dimer **4** revealed an anisotropy barrier of the two connected SMMs slightly lower with respect to the pristine $TbPc_2$ and a less-pronounced hysteretic behavior. This can be rationalized considering that the length of the aliphatic spacer used to connect the two magnetic centers prevents any significant coupling effect and introduces a LF strain. Nevertheless, the nontrivial retaining of the magnetic properties allows identifying the ADMET-based protocol as a valid candidate for the realization of $TbPc_2$ 1D structures. Thus, to improve the performances of the connected $TbPc_2$ molecules, an

DOI: 10.1021/acsomega.6b00546
ACS Omega 2017, 2, 517−521

optimization of the reaction and the use of highly conjugated chains will be necessary.

EXPERIMENTAL SECTION

Unless stated otherwise, reactions were conducted in flame-dried glassware under an atmosphere of argon using anhydrous solvents (either freshly distilled or passed through activated alumina columns). All commercially obtained reagents were used as received unless otherwise specified. Silica column chromatography was performed using silica gel 60 (Fluka 230−400 mesh or Merck 70−230 mesh). ^{1}H NMR spectra were obtained using a Bruker AVANCE 300 (300 MHz) and a Bruker AVANCE 400 (400 MHz) spectrometer at 25 °C. All chemical shifts (δ) were reported in ppm relative to the proton resonances resulting from incomplete deuteration of the NMR solvents. High-resolution MALDI-TOF was performed on an AB SCIEX MALDI TOF−TOF 4800 Plus (matrix: a-cyano-4-hydroxycinnamic acid). UV−vis spectra were collected using a Thermo Scientific Evolution 260 Bio spectrophotometer equipped with a Peltier water-cooled cell changer device, using matched quartz cells of 1 cm path length. Compound **1** was prepared according to modified published procedures.[24]

Pc(OC$_9$H$_{18}$CH=CH$_2$) (2). Phthalocyanine **1** (0.131 g, 0.09 mmol) was suspended in 10 mL of DMF, and K_2CO_3 (0.025 g, 0.18 mmol) was added, followed by a catalytic amount of KI. After the addition of 11-bromo-1-undecene (0.03 mL, 0.14 mmol), the mixture was heated at 120 °C for 3 h. The reaction was cooled and the solvent was removed under reduced pressure. Flash column chromatography (hexane/CH_2Cl_2 4:6) afforded pure phthalocyanine **2** (0.082 g, 0.05 mmol, 57%) as a green solid. ^{1}H NMR ($CDCl_3$, 400 MHz): δ (ppm) = 8.78−8.10 (m, 8H), 7.57−7.26 (m, 25H), 5.88 (m, 1H), 5.04 (m, 2H), 4.37 (m, 2H), 2.12 (m, 4H), 1.72−1.28 (m, 66H), −3.41 (bs, 2H). UV−vis: λ_{max} ($CHCl_3$) = 703, 670, 641, 602, 396, 346 nm. MALDI-TOF: calcd for $C_{103}H_{110}N_8O_7$ $[M]^+$ m/z = 1571.853; found m/z = 1571.757.

Tb[Pc(OC$_9$H$_{18}$CH=CH$_2$)]$_2$ (3). Phthalocyanine **2** (0.083 g, 0.052 mmol) was dispersed in 0.3 g of *n*-hexadecanol. [Tb(acac)$_3$]·nH$_2$O (0.012 g, 0.026 mmol) and lithium methoxide (0.006 g, 0.156 mmol) were added, and the mixture was heated at 180 °C for 1 h. After cooling, hexane was added and the mixture was filtrated. The solvent was removed under reduced pressure, and the crude was purified by flash column chromatography (gradient from hexane/CH_2Cl_2 1:1 to hexane/CH_2Cl_2 3:7). Further purification by preparative TLC (hexane/CH_2Cl_2 1:1) afforded product 3 as a green solid (0.041 g, 0.012 mmol, 49%). UV−vis: λ_{max} ($CHCl_3$) = 915, 681, 614, 490, 364, 330 nm. MALDI-TOF: calcd for $C_{206}H_{216}N_{16}O_{14}Tb$ $[M]^+$ m/z = 3298.600; found m/z = 3298.525.

Metathesis Oligomerization of 3. *Method a*: $TbPc_2$ **3** (0.011 g, 0.003 mmol) was dissolved in 1.5 mL of freshly distilled and degassed CH_2Cl_2. Second-generation Grubbs catalyst (0.14 mg, 5 mol %) was added, and the mixture was stirred at room temperature overnight. The reaction was quenched with MeOH (100 mL), and the green precipitate was filtered and dried. *Method b*: $TbPc_2$ **3** (0.080 g, 0.024 mmol) was dissolved in 1 mL of freshly distilled and degassed DCE. Second-generation Grubbs catalyst (0.001 g, 5 mol %) was added, and the mixture was stirred at room temperature for 3 days. The reaction was quenched with MeOH (100 mL), and the green precipitate was filtered and dried. $TbPc_2$ dimer **4**, isolated by preparative TLC (hexane/CH_2Cl_2 1:1), was obtained as a green solid (0.018 g, 0.003 mmol, 23%). UV−vis: λ_{max} ($CHCl_3$) = 916, 681, 616, 493, 363, 330 nm. MALDI-TOF: linear scan mode, calcd for $C_{410}H_{428}N_{32}O_{28}Tb_2$ $[M]^+$ m/z = 6569.2; found m/z = 6569.4.

Magnetic Measurements. The dc magnetic characterization was performed using a Quantum Design MPMS SQUID magnetometer. The ac characterization at frequency between 0.1 and 1000 Hz (Figures S10−S11 and S14−S15) was performed using the same instrument used for dc. The high-temperature−high-frequency ac measurements were performed using a Quantum Design PPMS (Figures S12−S13 and S16−S17). The investigated sample was a pellet composed by 8.1 mg of microcrystalline powder, to avoid in-field orientation of the microcrystallites.

ASSOCIATED CONTENT

Supporting Information

The Supporting Information is available free of charge on the ACS Publications website at DOI: 10.1021/acsomega.6b00546.

NMR, MALDI, and UV−vis spectra; dc and ac magnetic measurements (PDF)

AUTHOR INFORMATION

Corresponding Author

*E-mail: enrico.dalcanale@unipr.it.

ORCID

Matteo Mannini: 0000-0001-7549-2124

Enrico Dalcanale: 0000-0001-6964-788X

Notes

The authors declare no competing financial interest.

ACKNOWLEDGMENTS

A.P. thanks INSTM for partial support of his scholarship. We thank Dr. Gianluca Paredi of SITEIA, University of Parma, for high-resolution MALDI-TOF MS analyses and Centro Intefacoltà di Misure "G. Casnati" of the University of Parma for the use of NMR facilities.

REFERENCES

(1) Layfield, R. A. Organometallic Single-Molecule Magnets. *Organometallics* **2014**, *33*, 1084−1099.

(2) Gatteschi, D.; Sessoli, R.; Villain, J. *Molecular Nanomagnets*; Oxford University Press: Oxford, 2006.

(3) Leuenberger, M. N.; Loss, D. Quantum computing in molecular magnets. *Nature* **2001**, *410*, 789−793.

(4) Mannini, M.; Pineider, F.; Danieli, C.; Totti, F.; Sorace, L.; Sainctavit, P.; Arrio, M. A.; Otero, E.; Joly, L.; Cezar, J. C.; Cornia, A.; Sessoli, R. Quantum tunnelling of the magnetization in a monolayer of oriented single-molecule magnets. *Nature* **2010**, *468*, 417−421.

(5) *See for instance*: Thiele, S.; Balestro, F.; Ballou, R.; Klyatskaya, S.; Ruben, M.; Wernsdorfer, W. Electrically driven nuclear spin resonance in single-molecule magnets. *Science* **2014**, *344*, 1135−1138.

(6) Ishikawa, N.; Sugita, M.; Ishikawa, T.; Koshihara, S.; Kaizu, Y. Lanthanide Double-Decker Complexes Functioning as Magnets at the Single-Molecular Level. *J. Am. Chem. Soc.* **2003**, *125*, 8694−8695.

(7) Ishikawa, N.; Sugita, M.; Okubo, T.; Tanaka, N.; Iino, T.; Kaizu, Y. Determination of Ligand-Field Parameters and f-Electronic Structures of Double-Decker Bis(phthalocyaninato)lanthanide Complexes. *Inorg. Chem.* **2003**, *42*, 2440−2446.

(8) Rinehart, J. D.; Long, J. R. Exploiting single-ion anisotropy in the design of f-element single-molecule magnets. *Chem. Sci.* **2011**, *2*, 2078−2085.

(9) Ganivet, C. R.; Ballesteros, B.; de la Torre, G.; Clemente-Juan, J. M.; Coronado, E.; Torres, T. Influence of Peripheral Substitution on the Magnetic Behavior of Single-Ion Magnets Based on Homo- and

DOI: 10.1021/acsomega.6b00546
ACS Omega 2017, 2, 517−521

Heteroleptic Tb^{III} Bis(phthalocyaninate). *Chem. – Eur. J.* **2013**, *19*, 1457–1465.
(10) Sessoli, R.; Gatteschi, D. Quantum tunneling of magnetization and related phenomena in molecular materials. *Angew. Chem., Int. Ed.* **2003**, *42*, 268–297.
(11) Ishikawa, N.; Sugita, M.; Wernsdorfer, W. Quantum Tunneling of Magnetization in Lanthanide Single-Molecule Magnets: Bis(phthalocyaninato)terbium and Bis(phthalocyaninato)dysprosium Anions. *Angew. Chem., Int. Ed.* **2005**, *44*, 2931–2935.
(12) Wernsdorfer, W.; Aliaga-Alcalde, N.; Hendrickson, D. N.; Christou, G. Exchange-biased quantum tunnelling in a supramolecular dimer of single-molecule magnets. *Nature* **2002**, *416*, 406–409.
(13) (a) Ferbinteanu, M.; Miyasaka, H.; Wernsdorfer, W.; Nakata, K.; Sugiura, K.-I.; Yamashita, M.; Coulon, C.; Clérac, R. Single-Chain Magnet $(NEt_4)[Mn_2(5\text{-}MeOsalen)_2Fe(CN)_6]$ Made of Mn^{III}–Fe^{III}–Mn^{III} Trinuclear Single-Molecule Magnet with an $S_T = {}^9/_2$ Spin Ground State. *J. Am. Chem. Soc.* **2005**, *127*, 3090–3099. (b) Lecren, L.; Wernsdorfer, W.; Li, Y. G.; Vindigni, A.; Miyasaka, H.; Clérac, R. One-Dimensional Supramolecular Organization of Single-Molecule Magnets. *J. Am. Chem. Soc.* **2007**, *129*, 5045–5051. (c) Roubeau, O.; Clérac, R. Rational Assembly of High-Spin Polynuclear Magnetic Complexes into Coordination Networks: the Case of a [Mn4] Single-Molecule Magnet Building Block. *Eur. J. Inorg. Chem.* **2008**, *28*, 4325–4342. (d) Miyasaka, H.; Takayama, K.; Saitoh, A.; Furukawa, S.; Yamashita, M.; Clérac, R. Three-Dimensional Antiferromagnetic Order of Single-Chain Magnets: A New Approach to Design Molecule-Based Magnets. *Chem. – Eur. J.* **2010**, *16*, 3656–3662. (e) Jeon, I.-R.; Clérac, R. Controlled association of single-molecule magnets (SMMs) into coordination networks: towards a new generation of magnetic materials. *Dalton Trans.* **2012**, *41*, 9569–9586. (f) Tsai, H.-L.; Yang, C.-I.; Wernsdorfer, W.; Huang, S.-H.; Jhan, S.-Y.; Liu, M.-H.; Lee, G.-H. Mn_4 Single-Molecule-Magnet-Based Polymers of a One-Dimensional Helical Chain and a Three-Dimensional Network: Syntheses, Crystal Structures, and Magnetic Properties. *Inorg. Chem.* **2012**, *51*, 13171–13180. (g) Ababei, R.; Pichon, C.; Roubeau, O.; Li, Y.-G.; Bréfuel, N.; Buisson, L.; Guionneau, P.; Mathonière, C.; Clérac, R. Rational Design of a Photomagnetic Chain: Bridging Single-Molecule Magnets with a Spin-Crossover Complex. *J. Am. Chem. Soc.* **2013**, *135*, 14840–14853. (h) Rigamonti, L.; Cotton, C.; Nava, A.; Lang, H.; Rüffer, T.; Perfetti, M.; Sorace, L.; Barra, A.-L.; Lan, Y.; Wernsdorfer, W.; Sessoli, R.; Cornia, A. Diamondoid Structure in a Metal–Organic Framework of Fe_4 Single-Molecule Magnets. *Chem. – Eur. J.* **2016**, *22*, 13705–13714.
(14) Malavolti, L.; Mannini, M.; Car, P.; Campo, G.; Pineider, F.; Sessoli, R. Erratic magnetic hysteresis of $TbPc_2$ molecular nanomagnets. *J. Mater. Chem. C* **2013**, *1*, 2935–2942.
(15) (a) Kahn, M. L.; Sutter, J.-P.; Golhen, S.; Guionneau, P.; Ouahab, L.; Kahn, O.; Chasseau, D. Systematic Investigation of the Nature of The Coupling between a Ln(III) Ion (Ln = Ce(III) to Dy(III)) and Its Aminoxyl Radical Ligands. Structural and Magnetic Characteristics of a Series of $\{Ln(organic\ radical)_2\}$ Compounds and the Related $\{Ln(Nitrone)_2\}$ Derivatives. *J. Am. Chem. Soc.* **2000**, *122*, 3413–3421. (b) Bogani, L.; Sangregorio, C.; Sessoli, R.; Gatteschi, D. Molecular Engineering for Single-Chain-Magnet Behavior in a One-Dimensional Dysprosium–Nitronyl Nitroxide Compound. *Angew. Chem., Int. Ed.* **2005**, *44*, 5817–5821. (c) Bernot, K.; Bogani, L.; Caneschi, A.; Gatteschi, D.; Sessoli, R. A Family of Rare-Earth-Based Single Chain Magnets: Playing with Anisotropy. *J. Am. Chem. Soc.* **2006**, *128*, 7947–7956. (d) Liu, R.; Li, L. C.; Wang, X. L.; Yang, P. P.; Wang, C.; Liao, D. Z.; Sutter, J. P. Smooth transition between SMM and SCM-type slow relaxing dynamics for a 1-D assemblage of $\{Dy(nitronyl\ nitroxide)_2\}$ units. *Chem. Commun.* **2010**, *46*, 2566–2568. (e) Sessoli, R.; Bernot, K. In *Lanthanides and Actinides in Molecular Magnetism*; Layfield, R. A., Murugesu, M., Eds.; Wiley-VCH Verlag & Co.: Weinheim, Germany, 2015; Chapter 4, pp 89–124 and references therein.
(16) (a) Rinehart, J. D.; Fang, M.; Evans, W. J.; Long, J. R. Strong exchange and magnetic blocking in N_2^{3-}-radical-bridged lanthanide complexes. *Nat. Chem.* **2011**, *3*, 538–542. (b) Rinehart, J. D.; Fang, M.; Evans, W. J.; Long, J. R. A N_2^{3-} Radical-Bridged Terbium Complex Exhibiting Magnetic Hysteresis at 14 K. *J. Am. Chem. Soc.* **2011**, *133*, 14236–14239. (c) Fang, M.; Bates, J. E.; Lorenz, S. E.; Lee, D. S.; Rego, D. B.; Ziller, J. W.; Furche, F.; Evans, W. J. $(N_2)^{3-}$ Radical Chemistry via Trivalent Lanthanide Salt/Alkali Metal Reduction of Dinitrogen: New Syntheses and Examples of $(N_2)^{2-}$ and $(N_2)^{3-}$ Complexes and Density Functional Theory Comparisons of Closed Shell Sc^{3+}, Y^{3+}, and Lu^{3+} versus $4f^9$ Dy^{3+}. *Inorg. Chem.* **2011**, *50*, 1459–1469.
(17) Wang, K.; Qi, D.; Wang, H.; Cao, W.; Li, W.; Liu, T.; Duan, C.; Jiang, J. Binuclear Phthalocyanine-Based Sandwich-Type Rare Earth Complexes: Unprecedented Two π-Bridged Biradical-Metal Integrated SMMs. *Chem. – Eur. J.* **2013**, *19*, 11162–11166.
(18) (a) Lindermark-Hamberg, M.; Wagener, K. B. Acyclic metathesis polymerization: the olefin metathesis reaction of 1,5-hexadiene and 1,9-decadiene. *Macromolecules* **1987**, *20*, 2949–2951. (b) Mutlu, H.; Montero de Espinosa, L.; Meier, M. A. R. Acyclic diene metathesis: a versatile tool for the construction of defined polymer architectures. *Chem. Soc. Rev.* **2011**, *40*, 1404–1445.
(19) Kimura, M.; Wada, K.; Ohta, K.; Hanabusa, K.; Shirai, H.; Kobayashi, N. Preparation of Ordered Stacked Phthalocyanine Polymers through Olefin Metathesis Reaction. *Macromolecules* **2001**, *34*, 4706–4711.
(20) Mannini, M.; Bertani, F.; Tudisco, C.; Malavolti, L.; Poggini, L.; Misztal, K.; Menozzi, D.; Motta, A.; Otero, E.; Ohresser, P.; Sainctavit, P.; Condorelli, G. G.; Dalcanale, E.; Sessoli, R. Magnetic behaviour of $TbPc_2$ single-molecule magnets chemically grafted on silicon surface. *Nat. Commun.* **2014**, *5*, No. 4582.
(21) Pushkarev, V. E.; Tolbin, A. Y.; Borisova, N. E.; Trashin, S. A.; Tomilova, L. G. A_3B-Type Phthalocyanine-Based Homoleptic Lanthanide(III) Double-Decker π-Radical Complexes Bearing Functional Hydroxy Groups: Synthetic Approach, Spectral Properties and Electrochemical Study. *Eur. J. Inorg. Chem.* **2010**, 5254–5262.
(22) Cosquer, G.; Pointillart, F.; Golhen, S.; Cador, O.; Ouahab, L. Slow Magnetic Relaxation in Condensed versus Dispersed Dysprosium(III) Mononuclear Complexes. *Chem. – Eur. J.* **2013**, *19*, 7895–7903.
(23) Casimir, H. B. J.; Du Pré, F. K. Note on the thermodynamic interpretation of paramagnetic relaxation phenomena. *Physica* **1938**, *5*, 507–511.
(24) (a) Tolbin, A. Y.; Pushkarev, V. E.; Tomilova, L. G.; Zefirov, N. S. Selective synthesis of clamshell-type binuclear phthalocyanines. *Mendeleev Commun.* **2009**, *19*, 78–80. (b) Polaske, N. W.; Lin, H.-C.; Tang, A.; Mayukh, M.; Oquendo, L. E.; Green, J. T.; Ratcli, E. L.; Armstrong, N. R.; Saaverda, S. S.; McGrath, D. V. Phosphonic Acid Functionalized Asymmetric Phthalocyanines: Synthesis, Modification of Indium Tin Oxide, and Charge Transfer. *Langmuir* **2011**, *27*, 14900–14909.

DOI: 10.1021/acsomega.6b00546
ACS Omega 2017, 2, 517–521